

Lawrence Berkeley National Laboratory

Recent Work

Title

THE EFFECT OF CONDENSATION IN THE BOUNDARY LAYER ON MASS TRANSFER FROM A ROTATING DISK PART II, EXPERIMENTAL

Permalink

<https://escholarship.org/uc/item/31h865t4>

Authors

Omberg, R.P.
Olander, D.R.

Publication Date

1970-10-01

c.2

RECEIVED
LAWRENCE
RADIATION LABORATORY

NOV 19 1970

LIBRARY AND
DOCUMENTS SECTION

THE EFFECT OF CONDENSATION
IN THE BOUNDARY LAYER ON MASS TRANSFER
FROM A ROTATING DISK
PART II, EXPERIMENTAL

R. P. Omberg and D. R. Olander

October 1970

AEC Contract No. W-7405-eng-48

TWO-WEEK LOAN COPY

*This is a Library Circulating Copy
which may be borrowed for two weeks.
For a personal retention copy, call
Tech. Info. Division, Ext. 5545*

LAWRENCE RADIATION LABORATORY
UNIVERSITY of CALIFORNIA BERKELEY

c.2

DISCLAIMER

This document was prepared as an account of work sponsored by the United States Government. While this document is believed to contain correct information, neither the United States Government nor any agency thereof, nor the Regents of the University of California, nor any of their employees, makes any warranty, express or implied, or assumes any legal responsibility for the accuracy, completeness, or usefulness of any information, apparatus, product, or process disclosed, or represents that its use would not infringe privately owned rights. Reference herein to any specific commercial product, process, or service by its trade name, trademark, manufacturer, or otherwise, does not necessarily constitute or imply its endorsement, recommendation, or favoring by the United States Government or any agency thereof, or the Regents of the University of California. The views and opinions of authors expressed herein do not necessarily state or reflect those of the United States Government or any agency thereof or the Regents of the University of California.

THE EFFECT OF CONDENSATION
IN THE BOUNDARY LAYER ON MASS TRANSFER
FROM A ROTATING DISK
PART II, EXPERIMENTAL

by

R.P. Omberg* and D.R. Olander

Inorganic Materials Research Division,
Lawrence Radiation Laboratory, and

Department of Nuclear Engineering,
University of California, Berkeley, Calif. 94720

ABSTRACT

The vaporization rate of chromium metal into an atmosphere of cold helium gas was measured in a rotating disk flow geometry. Gas conditions were 1 atm pressure and temperatures of 300°K and 600°K. The disk temperature was varied from 1630°K to 1760°K.

At the lowest disk temperatures, the rates appeared to approach the values predicted by isothermal convection-diffusion theory. At higher temperatures, the measured rates were considerably greater than those predicted by simple mass transfer considerations and were reduced when the helium temperature was increased. These observations suggest that condensation of metal vapor in the boundary layer was accelerating the vaporization rate. At the highest disk temperature investigated, the observed rate was a factor of 10 greater than the rate predicted from isothermal rotating disk theory. A difference of this magnitude is expected for kinetically unhindered condensation in the boundary layer (i.e., the metal partial pressure follows the temperature profile according to the vapor pressure curve). The theoretical treatment of Part I, which was based upon classical nucleation theory, does not predict rate enhancements this large.

*Present address: WADCO Corporation, a Subsidiary of Westinghouse Corporation, Richland, Washington.

I. INTRODUCTION

The effect of condensation in the thermal boundary layer on the mass transfer rate from a hot metal surface was investigated experimentally. The vaporization rate of a hot metal disk rotating in a cold inert gas environment was measured at temperatures and angular velocities calculated to produce nucleation in the boundary layer. It was shown theoretically in a previous paper¹ that the formation of nuclei should promote condensation and thus increase the vaporization rate. Experimental verification of the effect of condensation on the vaporization rate was sought.

Turkdogan and Mills² measured roughly the vaporization rate of molten iron spheres surrounded by helium and cooled by natural convection. The spheres were heated by an induction coil and were suspended by levitation within the coil. The measured rates were approximately three times greater than the isothermal, diffusion-limited, condensation-free value calculated from semi-empirical correlations. This factor of three increase in the vaporization rate agreed qualitatively with the predictions of a "critical supersaturation" model proposed by Turkdogan.³ Their experiments, however, were not conducted with the express purpose of testing the theory of condensation enhancement of the vaporization rate. Therefore, no particular care was taken to insure that certain necessary boundary conditions were attained in the experiment. Thus, their experimental results should be considered in a qualitative rather than a quantitative sense.

Elenbaas⁴ measured the vaporization rate of a resistance-heated tungsten filament wound in the shape of a coil and surrounded by krypton gas. The filament was cooled by natural convection. He found no enhancement in the vaporization rate due to condensation. The calculated concentration and thermal diffusion fluxes obtained from stagnant film theory accounted for nearly all of the measured flux. The results Elenbaas obtained agreed with a theory based upon the assumption that drops formed by nucleation are transported only by diffusion and do not penetrate the outer edge of the stagnant layer. According to this model, the enhancement is zero, and condensation in the boundary layer has no effect on the vaporization rate.⁵

We have attempted to determine the effect of condensation in the thermal boundary layer more precisely than in the aforementioned studies in an effort to resolve the contradiction between Turkdogan's and Elenbaas' conclusions. To this end, the vaporization rate with condensation was measured in a rotating disk system. The advantage of the rotating disk system is that the measured rate can be compared with an exactly calculated, theoretical rate both with and without condensation. The concentration and temperature profiles can be determined from first principles and hence, the condensation-free vaporization rate calculated exactly.^{6,7,8} In addition, diffusion, convection, and growth of the drops formed by homogeneous nucleation in the boundary layer can be exactly described by a set of ordinary differential equations.¹ The solution of these equations gives the condensation-enhanced vaporization rate.

The rotating disk also has the advantage of being a precise experimental tool. For example, Olander⁹ found very good agreement between theory and experiment while studying the diffusion-limited

chemical reaction between iodine and germanium at moderate temperatures (approximately 600°K). Olander and Schofill¹⁰ found very good agreement between theory and experiment while studying the diffusion-limited chemical reaction between oxygen and molybdenum at very high temperatures (up to 2000°K). Other studies^{7,8} have also shown the exactness of this tool.

In this experiment, the material vaporized was chromium and the environment was cool helium. The disk was heated by induction. The vaporization rate was measured over a temperature range of approximately 100°K at approximately 1700°K.

II. DESCRIPTION OF THE EXPERIMENT

The rotating disk has what is called a "uniformly accessible surface." This is a term which is used to describe the experimental and theoretical fact that the mass flux leaving the disk, i.e., the vaporization rate, is independent of position on the disk. Because of this position-independence, the vaporization rate is obtained in an experiment simply by dividing the mass loss of the disk by its cross-sectional area and by the time over which the mass loss occurred. The primary problem is to obtain an accurately measurable mass loss in a reasonable amount of time. Some of the factors which affect this objective are described below.

(1) Selection of the Disk Material

The primary requirement of the disk material is that it has a sufficiently high vapor pressure while still solid in order to obtain a mass loss large enough to be measured. The material must also be relatively inert in order to prevent reactions with other elements in the system from obscuring the mass loss caused by vaporization. For example, a chemical reaction between the disk and the crucible at the temperatures of this experiment can easily produce a large mass change in the disk. Also, simple diffusion of the crucible elements into the disk can be a large source of error. A reaction can also occur with impurities in the inert gas stream. Any one, or a combination of all of these, can easily introduce errors much larger than the value intended to be measured.

Iron was initially tried because it is machinable by conventional methods. However, the vapor pressure over the solid is not particularly large and specimens had to be operated very close to their

melting point to obtain a measurable mass loss. Iron has a phase transition near its melting point where properties such as the specific heat change significantly. This caused the temperature of the disk to change quite rapidly even for minor fluctuations in the input power from the induction heater. As a consequence, the disks invariably melted. Thus iron was discarded and chromium was selected. Chromium has a very satisfactory vapor pressure as a solid (8 torr at the melting point of 2120°K).¹¹ However, chromium is considerably more difficult to fabricate than iron. Disks had to be spark-cut from flakes, which limited the amount of data taken because of the considerable effort required to prepare each sample.

(2) Equipmental Apparatus

The equipment is shown in Figures 1 and 2. The disk was contained in a boron nitride crucible which was attached to a tantalum shaft. A thin tungsten liner was placed between the chromium and the boron nitride in order to prevent a chemical reaction (the reaction between tungsten and boron nitride is much smaller than that between chromium and boron nitride). A synchronous motor drove the shaft through a bearing block, which was water-cooled to prevent overheating of the bearings. The shaft was $\frac{1}{4}$ inch in diameter and extended ~ 3 in. above the water-cooled bearing block. Shorter shafts could not be used because of the heat conducted from the hot disk down the shaft to the bearings and motor. The boron nitride holder was approximately one centimeter high by slightly more than one centimeter in diameter at its top. The motor was driven at constant speed by an audio-oscillator connected to a power amplifier. The oscillator provided a variable frequency

source to control the motor speed and the amplifier supplied the power necessary to drive the motor. The system was designed to run at speeds between 3,000 and 15,000 rpm. The chromium disk, along with the boron nitride holder, tantalum shaft, and synchronous motor, were enclosed in a large quartz tube. The coils of an induction heater were placed outside the quartz enclosure and encircled the chromium disk. The interior of the tube during a run was filled with a 96% He - 4% H₂ gas mixture. This atmosphere was sufficiently reducing to prevent oxide formation on the disk surface.

The helium-hydrogen mixture was treated by a gas purification system prior to entering the apparatus. The gas passed through a packed filter of pyrex filtering fiber, then through two "Drierite" dessicators, and finally through another packed pyrex filter to remove dust particles. All lines leading from the bottled gas supply to the quartz enclosure and the gas purification system were constructed entirely of stainless steel which had been chemically polished to remove surface impurities. The only exception was a very short piece of copper line where the metal-to-quartz junction was made. The gas purification system and connecting lines were kept in an argon atmosphere whenever the system was not operating. These precautions were necessary to prevent impurities from entering the system and later depositing on the hot chromium surface.

Upon entering the quartz tube, the gas mixture was cooled with a water-cooled heat exchanger. The heat exchanger prevented the gas from being heated by the quartz enclosure as it traveled toward the disk. The temperature of the quartz enclosure was higher than ambient because the hot disk radiated to it. By cooling the gas, a precisely known boundary condition at the outer edge of the boundary layer was obtained.

(3) Fabrication of the Disk

The chromium disks were spark-cut from electrolytically formed chromium flakes containing less than 50 ppm metallic impurities and 500 ppm of dissolved gas. The disks were approximately one centimeter in diameter by one millimeter thick. After spark-cutting, the entire disk surface was chemically cleaned with hydrochloric acid at 35°C for several minutes. The surface to be vaporized was then polished on a rotary wheel with silicon-carbide paper, beginning with #380 and proceeding to #600. The disk surface was finally finished with six micron powder. The tungsten liners were cleaned by hand with #400 silicon-carbide paper. The disk, liners, and crucible were finally ultrasonically cleaned with acetone and methanol. They were then stored in a vacuum dessicator until used.

(4) Experimental Procedure

The apparatus was assembled for an experiment by placing the weighed tungsten liner--chromium disk combination into the boron nitride crucible, and then threading the crucible onto the tantalum shaft. The quartz tube was placed around the disk assembly and the helium-hydrogen supply connected. The gas flow rate was adjusted to a value equal to that pumped by the disk plus a small additional amount to insure that the system operated at a positive pressure. The additional gas flow was calculated to be small enough not to affect the velocity profiles around the disk significantly.^{6,7}

To begin the experiment, the synchronous motor and induction heater were turned on and the disk speed and the temperature were adjusted to the values intended for the run. The runs lasted from

twenty minutes to one hour; the duration of an experiment was chosen so that the total mass loss from the disk would be between one and ten milligrams. Above ten milligrams the amount of material vaporized was so large that the upper surface of the disk receded below the upper surface of the crucible, which disturbed the boundary layer to such an extent that chromium condensed in large quantities on the disk edge adjacent to the boron nitride crucible. At weight losses below one milligram the accuracy of the measurement began to be affected by the small reaction which took place between the tungsten liner and the boron nitride. The amount of metal vaporized was determined by the difference between the initial and final weights of the chromium disk and tungsten liner. The tare weight of the tungsten liner was included because after the run, it was firmly attached to the chromium disk by a diffusion bond.

The temperatures were measured with an optical pyrometer which viewed the disk through a right-angle prism and an optical flat located on top of the quartz enclosure shown in Fig. 1. The temperature correction due to these components was determined by calibration with a tungsten lamp.

A small hole was spark cut in the center of the disk. The hole had a length-to-diameter ratio of approximately unity, and although it was not a perfect block body, it did have an emissivity considerably higher than the chromium surface. This hole was used to determine the emissivity of the disk surface by the method outlined in the appendix.

The disk temperature during the run was recorded, and adjusted if necessary, approximately once every minute. The temperature variation during the run at any point on the disk could be held to less than $\pm 5^{\circ}\text{C}$ by manually adjusting the power applied to the induction coil. Readings were taken at three different radial positions: the center ($r/r_0 \approx 0$),

halfway between the center and the edge ($r/r_0 \approx 1/2$), and at the edge ($r/r_0 \approx 1$). The variation from the center of the disk to the edge was usually on the order of 15°C . The average temperature at the three radial positions for the run was taken as the simple time-average of all the temperatures recorded at that position during the run. The apparent temperatures were corrected for a surface emissivity at 0.50 by Eq (A) of the appendix.

The vapor pressure was determined by fitting a parabola through the three radial temperatures $T(0)$, $T(1/2)$ and $T(1)$. Since the mass loss rate is proportional to the vapor pressure and to the incremental area over which the vapor pressure exists, the average vapor pressure over the disk surface was determined by:

$$\bar{p}_v = \frac{2}{r_0} \int_0^{r_0} r p_v [T(r)] dr$$

vapor pressures were taken from ref. 11.

(5) Parameters Studied

Three different sets of runs were made. In the first set, the rotational speed of the disk was held constant at 12,000 rpm and the temperature varied from 1630°K to 1760°K . These experiments determined the effect of temperature upon the vaporization rate at constant rotational speed.

In the second set, the temperature was held constant at $1730^\circ\text{K} \pm 5^\circ\text{K}$ and the speed varied from 4200 rpm to 12,000 rpm. This set showed the effect of rotational speed on the vaporization rate at constant temperature.

The third set consisted of three runs at 12,000 rpm with a resistance heater replacing the inlet gas heat exchanger (see drawing of apparatus in ref. 10). The incoming gas was preheated to approximately 600°K by the heater, which increased the temperature and the equilibrium vapor pressure in the boundary layer. The supersaturation was thereby reduced and the amount of material condensing should then also be reduced if nucleation were in fact occurring.

For all the experimental runs, the Grashoff number divided by the Reynolds number squared for the disk was held to less than 0.05. In most cases it was on the order of 0.002. This insured that the effect of natural convection was small.¹² The flow was laminar.

III. RESULTS AND DISCUSSION

(1) Condition of the Surface

A typical chromium disk and boron nitride crucible after an experiment are shown in Fig. 3. The reflection of the pennies in the disk shows that the surface is both shiny and free from surface impurities which could have affected the vaporization rate tremendously.

Figures 4 and 5 are typical photomicrographs of the disk surface (magnification 100X) before and after an experiment. Figure 4 was taken before the run and shows a surface distinguished only by light polishing scratches. Figure 5 was taken after the run and shows the large grains which grow in the disk at high temperatures.

(2) Effect of Gas Temperature

Vaporization rates are shown in Table 1 and plotted as a function of disk temperature in Fig. 6. With the bulk gas at 300°K, measurements were made for disk temperatures from 1630°K to 1760°K. The points show very little scatter. The two points denoted by upward triangles were taken with the inlet gas heated to approximately 600°K by a preheating furnace. These points lie below the data taken with the inlet gas temperature of 300°K, indicating that nucleation was in fact occurring in the boundary layer. The point denoted by a downward triangle was taken with the gas preheating furnace installed but at zero power. This was done to determine whether the measurement of the disk temperature was affected simply by the physical presence of the heater directly above the disk. The proximity of this point to the line drawn through the other 300°K inlet gas points shows the effect to be small.

(3) Effect of Disk Temperature

The chief characteristic of the data shown in Fig. 6 is the rapid increase in the vaporization rate over a small temperature range from 1630°K to 1650°K followed by a gradual increase from 1650°K to 1760°K. The theoretical no-condensation and bulk equilibrium condensation vaporization rates calculated by the methods described in ref. 1 are also shown in the figure. It can be seen that as the disk temperature is increased, the experimental rate proceeds from the vicinity of the no-condensation line to the vicinity of the bulk equilibrium condensation line. The vaporization rate could not be measured below 1630°K, for two reasons. First, the errors in the experiment became a significant fraction of the mass loss due to vaporization at these temperatures. Second, the vaporization rate is changing quite rapidly with temperature in this region and so small errors in temperature measurement become quite important.

At the high temperature end, the data approach and eventually exceed the bulk equilibrium condensation curve. The reason for observed rates greater than the theoretical maximum rate is believed to be due to the inaccurate knowledge of the properties of the metal which determine the calculated rate.

The experimental vapor pressure data given in the literature scatters widely. Nesmeyanov¹¹ surveys most of the vapor pressure data available for the elements. Chromium has one of the better known vapor pressures and yet the data Nesmeyanov presents scatter by $\pm 50\%$. In addition, all the reliable data that Nesmeyanov presents for chromium are at 1550°K and below. Thus there is no vapor pressure data in the range in which the present experiments were conducted. Our experiments were on the average 150°K above the nearest data, and vapor pressures had to

be obtained by an extrapolation formula given by Nesmeyanov. For chromium at 1800°K, the vapor pressure recommended by Fultgren et al.¹³ is about two-thirds of Nesmeyanov's recommended value. This value, however, falls within the error band of $\pm 50\%$ for Nesmeyanov's data.

The second source of error in this experiment is in the measurement of the surface emissivity. If the surface emissivity were in fact 0.43 as suggested by the values reported in ref. 14 instead of the value of 0.50 measured here, all the data points in Fig. 6 would be shifted to a temperature approximately 15°K higher.

The effect of the possible emissivity and vapor pressure errors are shown in Fig. 7. The shaded areas around the no-condensation and bulk equilibrium condensation lines indicate the uncertainty in them due to scatter in the literature vapor pressures. The band denoted by $\Delta\epsilon_s$ represents the spread in the best line through the data due to emissivity variation from 0.50 to 0.43. The lower emissivity increases the difference between the brightness and true temperatures, and also improves agreement between equilibrium condensation theory and the data. The shaded area between the two lines indicates the error in the data due to a possible error in the emissivity.

The theoretical solutions¹ for constant drop diffusivity and variable drop diffusivity are also plotted in Fig. 6. These curves definitely fall below the bulk equilibrium condensation line and the measured data. This indicates that the monomer sink, and likewise the drop concentrations, calculated by the method described in ref. 1 were less than those actually existing in the boundary layer. The Becker-Doring-Zeldovich expression for the nucleation rate was used in our calculations because of the agreement with the diffusion chamber experi-

ments of Katz and Ostermier.¹⁵ However, the validity of classical nucleation theory is currently in dispute.¹⁶⁻¹⁹ Lothe and Pound¹⁹ have developed an expression for the nucleation rate which includes quantum-mechanical corrections to the classical expression which change the nucleation rate by a factor of 10^{17} . A change of this magnitude would definitely increase the droplet concentration and the monomer sink, and hence increase the calculated vaporization rate. Several attempts to compute vaporization rates using the Lothe-Pound expression were made. However, the nucleation rate calculated from the Lothe-Pound theory was an extremely sensitive function of the monomer concentration and numerical problems arose because the monomer concentration could not be interpolated between points with sufficient accuracy. However, if the calculations could be made, the Lothe-Pound nucleation rate expression should increase the calculated vaporization rate. This change is in the correct direction because an increase in the calculated nucleation rate will increase the rate of removal of monomer from the vapor phase.

(4) Effect of Disk Speed

Figure 8 shows a set of five points taken at an approximately constant temperature of $\sim 1730^\circ\text{K}$ with angular velocities from 4200 rpm to 12,000 rpm. The vaporization rate is plotted against the square root of the angular velocity. The figure shows the measured vaporization rate to be a linear function of the square root of the angular velocity and to pass through the origin. This type of behavior would be expected if vaporization were occurring either at the bulk equilibrium condensation rate or at the no-condensation rate.¹ If the vaporization rate is not at either limiting value, then the rate cannot be proportional to the square root of the angular velocity. This parameter occurs in the source term of the diffusion equation and is not removed by non-

dimensionalization. Thus Fig. 8 is consistent with the interpretation that vaporization is occurring at the bulk equilibrium condensation rate. Second, the figure shows that true rotating disk behavior was obtained in the boundary layer. One datum in Fig. 8 falls far below the others; something was clearly wrong in this measurement but what it was is unknown.

(5) Thermal Diffusion

The theoretical lines in the Fig. 6 were calculated neglecting property variations and thermal diffusion. Property variations were neglected because the diffusion coefficient of chromium through helium is approximately proportional to temperature squared and so the effect is small.²⁰ Thermal diffusion was neglected because the Lennard-Jones parameters for chromium-helium and iron-argon are very similar and ref. (20) shows thermal diffusion to be negligible in the iron-argon system. Moreover, even at the considerably higher temperature of 3200°K, Elenbaas⁴ found the affect of thermal diffusion for tungsten through krypton to be only 18% of the ordinary diffusion current. Thus the affect of thermal diffusion should be small compared to the variations involved in Fig. 6.

(6) Comparison with Other Data

Figure 9 shows the present data and Turkdogan's data³ on the same graph, even though the results are not strictly comparable because the present data are for chromium and Turkdogan's are for iron. However, these two metals are quite similar. Although, the flow geometries are different in the two experiments, the ratio of vaporization rates with and without boundary layer condensation should be similar. The composite plot reveals two basic trends. First, at low temperatures, the vaporization rate rises from the no-condensation

value to the equilibrium value as the temperature increases. Second, at higher temperatures, the vaporization rate again approaches the no-condensation rate as the temperature is increased because the latent heat released by the large quantity of condensing vapor lowers the bulk equilibrium line. The fact that Turkdogan's data in general follow this line was pointed out by Hills and Szekeley²¹ and also by Rosner and Epstein.²²

IV. CONCLUSIONS

Condensation enhancement was measured in rotating disk boundary layer. The vaporization rate rose rapidly from near the condensation-free value to the bulk equilibrium condensation value over a small temperature range.

At low surface temperatures no condensation enhancement is obtained because the system is close to the isothermal state. The absence of nucleation-condensation effects at low disk temperatures is in accord with the theoretical model presented in ref. 1.

As the disk temperature is increased, condensation enhancement occurs and the vaporization rate proceeds to the value determined by the equilibrium vapor pressure and the temperature profile. The rate calculated by the methods of ref. 1 are not in agreement with this observation if the classical Becker-Doring-Zeldovich nucleation expression is accepted. Although calculations could not be carried out using the Lothe-Pound expression, it is felt that the calculated vaporization rate which would be obtained with this nucleation theory would provide better agreement between experiment and theory.

As the surface temperature is increased further, the vaporization rate again approaches the condensation-free rate; this is because the heat released by the larger amount of vapor condensing in the boundary layer tends to make the system more isothermal.

Acknowledgement

This work was carried out under the auspices of the U.S. Atomic Energy Commission.

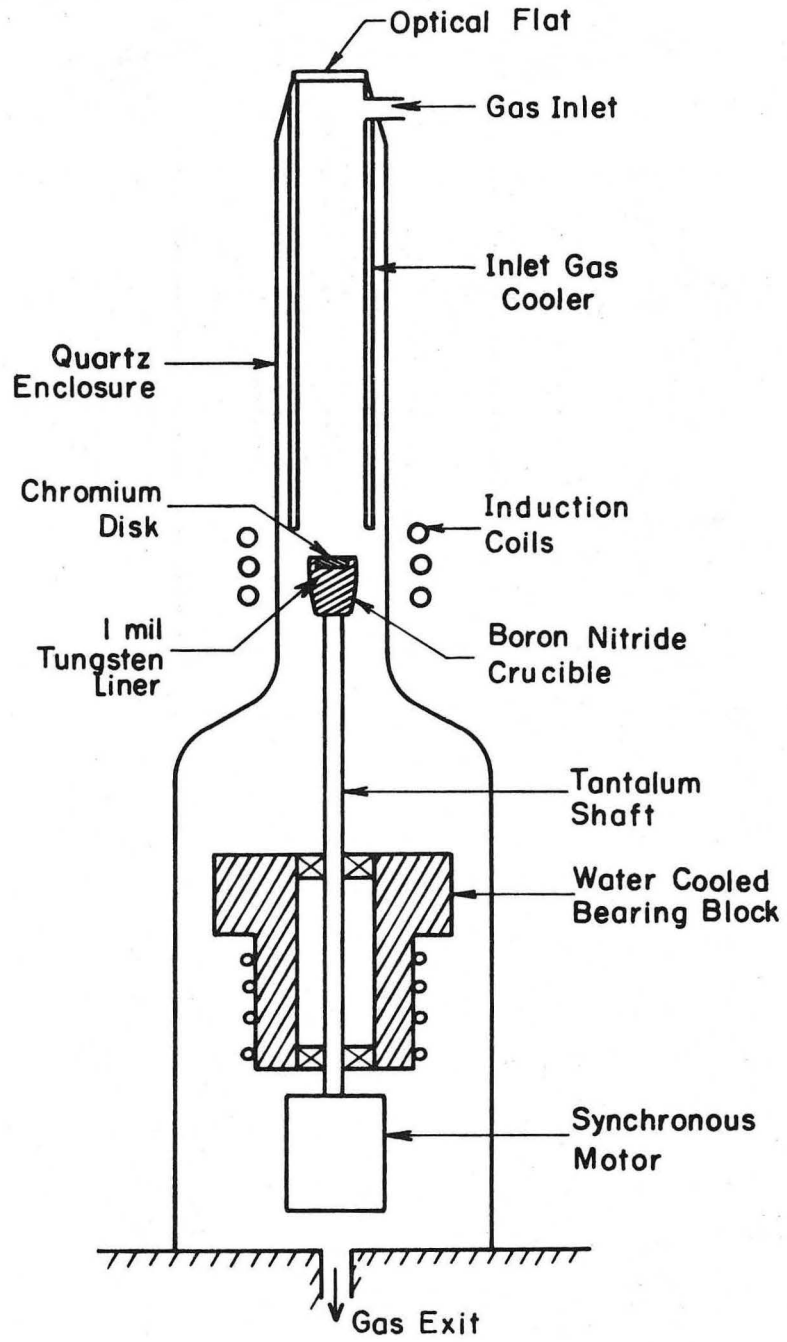
V. REFERENCES

- (1) Omberg, R.P. and D.R. Olander, submitted to Phys. of Fluids.
- (2) Turkdogan, E.T. and K.C. Mills, Trans. AIME, 230, 750 (1964).
- (3) Turkdogan, E.T., Trans. AIME, 230, 740 (1964).
- (4) Elenbaas, W., Phillips Research Reports, 22, 5 (1967).
- (5) Elenbaas, W., Phillips Research Reports, 22, 1 (1967).
- (6) Schlichting, H., Boundary Layer Theory, 4th ed., McGraw-Hill, New York, 1960, p. 85.
- (7) Dorfman, L.A., Hydrodynamic Resistance and the Heat Loss From Rotating Solids, Oliver and Boyd, Edinburg and London, 1963, (translated from Russian).
- (8) Levich, V.G., Physicochemical Hydrodynamics, Prentice-Hall, New Jersey, 1966, (translated from Russian).
- (9) Olander, D.R., Ind. and Eng. Chem. Fund., 6, 178 (1967).
- (10) Olander, D.R. and J. Schofill, Met. Trans., 1, (1970).
- (11) Nesmeyanov, A.N., Vapor Pressure of the Chemical Elements, Elsevier Publishing Co., New York, 1963, (translated from Russian).
- (12) Kreith, F., Principles of Heat Transfer, International Textbook, Scranton, Pa., 1958.
- (13) Hultgren, R., R.L. Orr, P.D. Anderson, and K.K. Kelley, Selected Values of Thermodynamic Properties of Metals and Alloys, John Wiley, New York, 1963.
- (14) Goldsmith, A., T.E. Waterman, and H.J. Hirschhorn, Handbook of Thermophysical Properties of Solid Materials, Vol. 1 - Elements, Pergamon Press, New York, 1961.
- (15) Katz, J.L., and B.J. Ostermier, J. Chem. Phys., 47, 478 (1967).
- (16) Feder, J., J.C. Russell, J. Lothe, and G.M. Pound, Adv. Physics, 15, 111 (1966).
- (17) Lothe, J., and G.M. Pound, J. Chem. Phys., 36, 2080 (1962).
- (18) Reiss, H., and J.L. Katz, J. Chem. Phys., 46, 2496 (1967).
- (19) Lothe, J., and G.M. Pound, J. Chem. Phys., 48, 1849 (1968).
- (20) Omberg, R.P., "The Effect of Condensation in the Boundary Layer on Mass Transfer from a Rotating Disk," UCRL-18577, Lawrence Radiation Laboratory, University of California, Berkeley (1969).

- (21) Hills, A.D.W., and J. Szekeley, Int. J. Heat and Mass Transfer, 12, 111 (1969).
- (22) Rosner, D.E., and M. Epstein, Trans. AIME, 242, 2355 (1968).
- (23) Eckert, E.R.G., and R.M. Drake, Heat and Mass Transfer, 2nd ed., McGraw-Hill, New York, 1959, p. 429.
- (24) Sparrow, E.M., L.U. Albers, and E.R.G. Eckert, J. of Heat Transfer, 84C, 73 (1962).

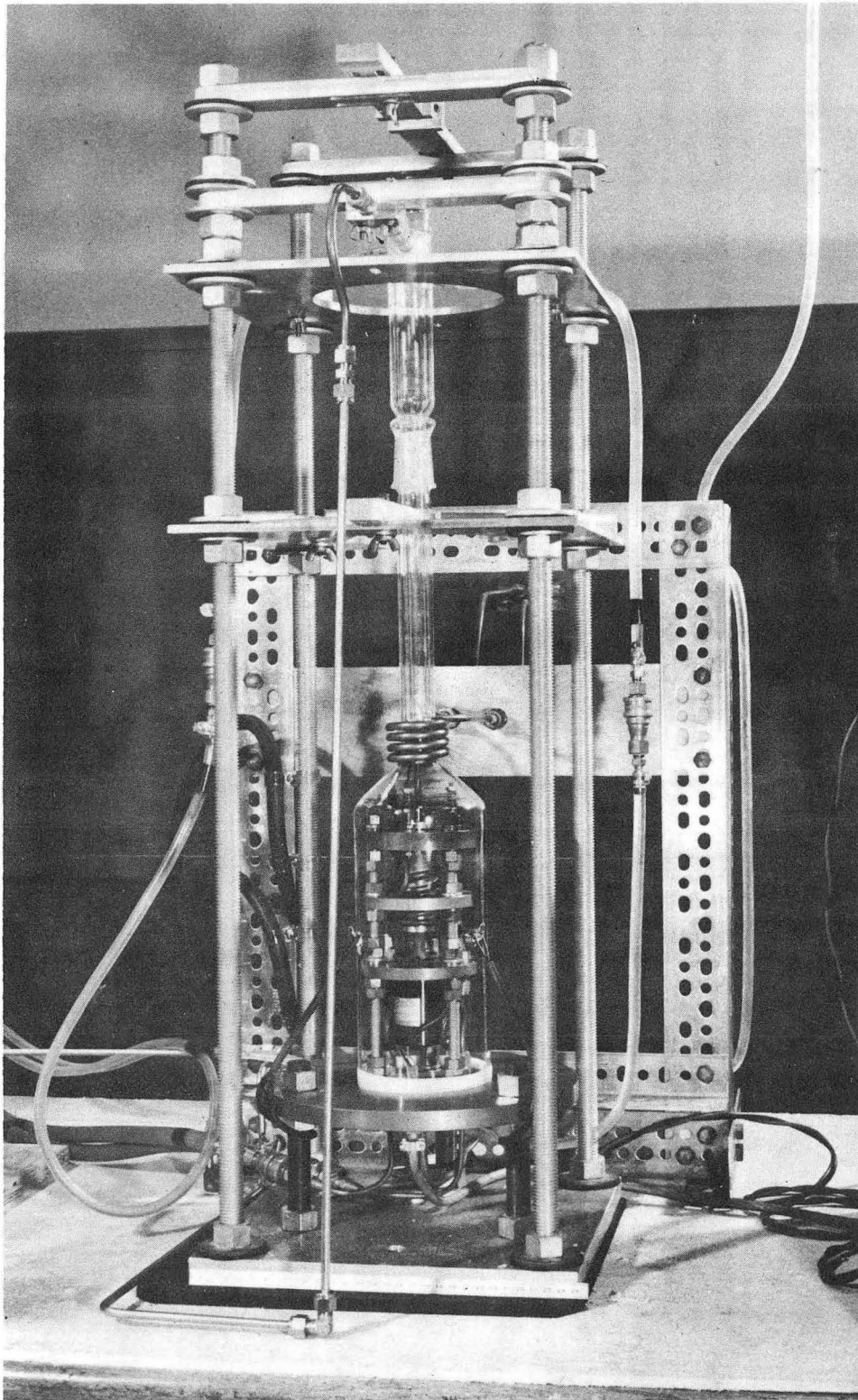
LIST OF FIGURES

1. Sketch of rotating disk apparatus.
2. Photograph of equipment .
3. Chromium disk after high temperature vaporization into helium-hydrogen gas mixture.
4. Polished disk surface before experiment.
5. Disk surface after vaporization experiment.
6. Effect of disk temperature on the vaporization rate. Curve A-- bulk equilibrium condensation; curve B--condensation with variable drop diffusivity; curve C--condensation with constant drop diffusivity; curve D--no condensation.
7. Effect of surface emissivity error on the experimental vaporization rates and of vapor pressure uncertainty on the predicted vaporization rates.
8. Effect of disk rotational speed on the vaporization rate at 1730°k.
9. Comparison of the present results with those of Turkdogan and Mills².



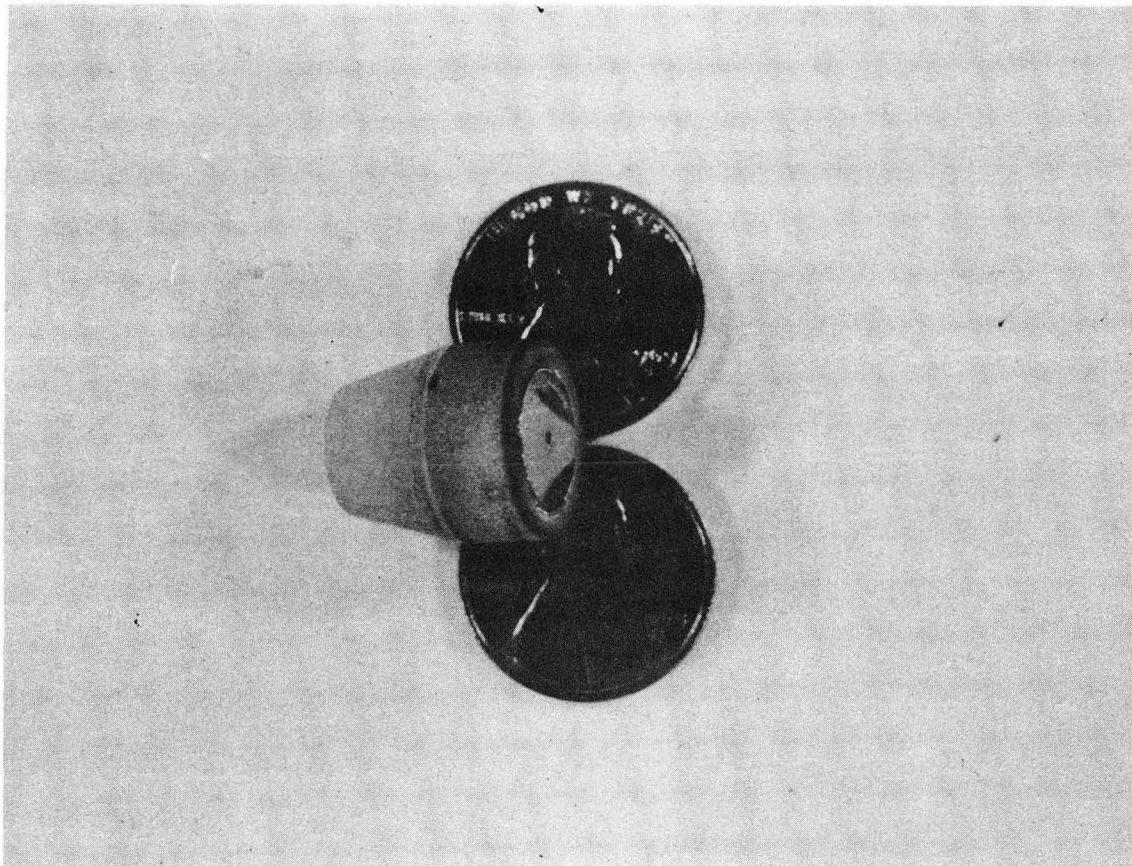
XBL 702-423

Fig. 1.



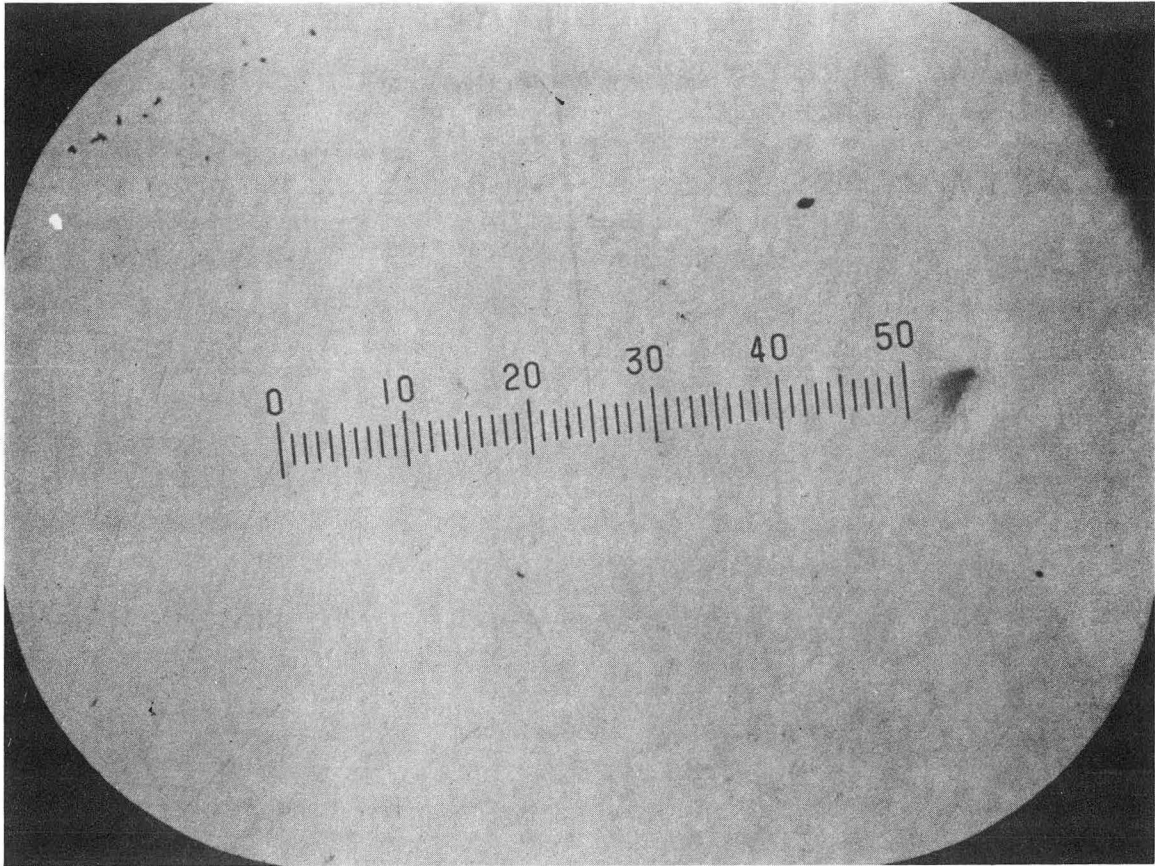
XBB698-5362

Fig. 2.



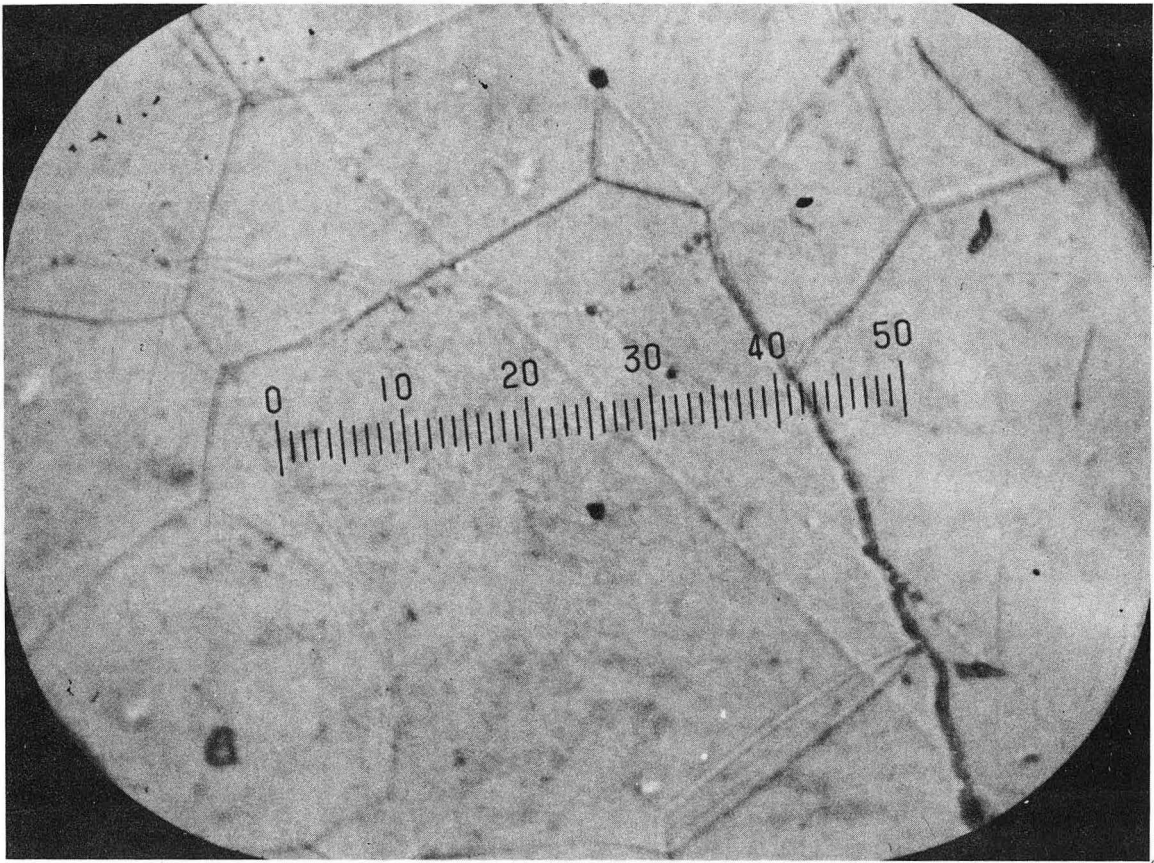
XBB698-5327

Fig. 3.



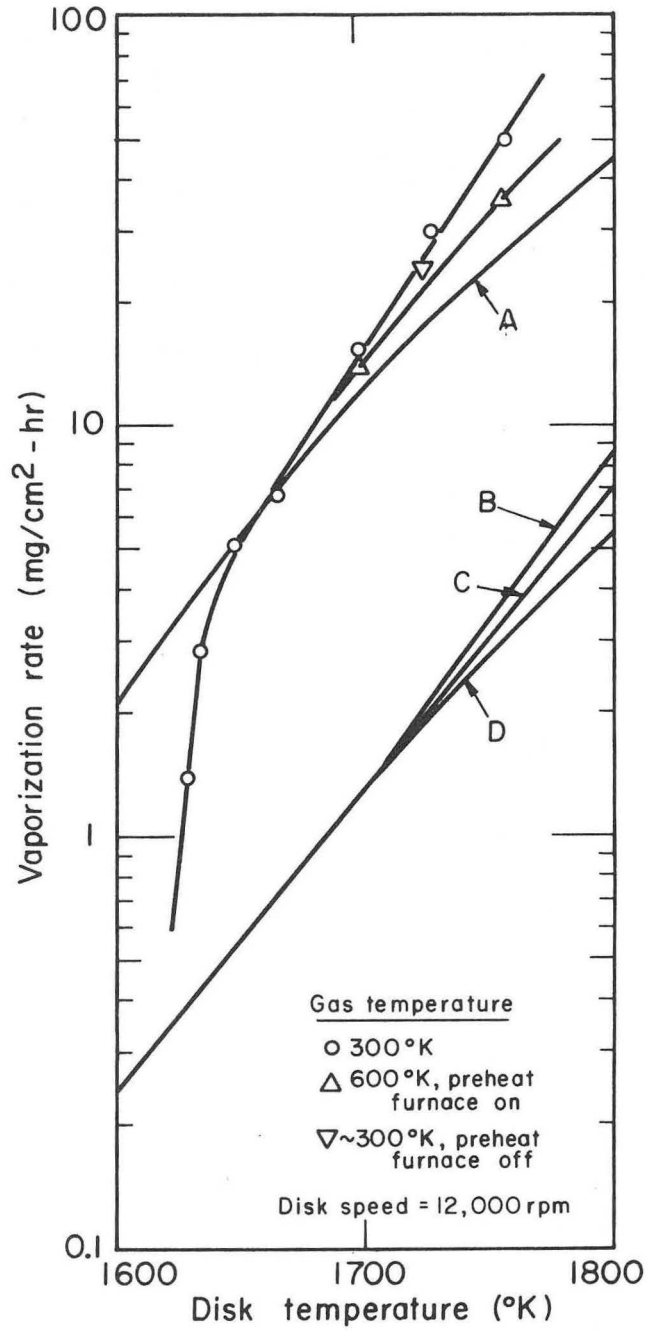
XBB698-5325

Fig. 4.



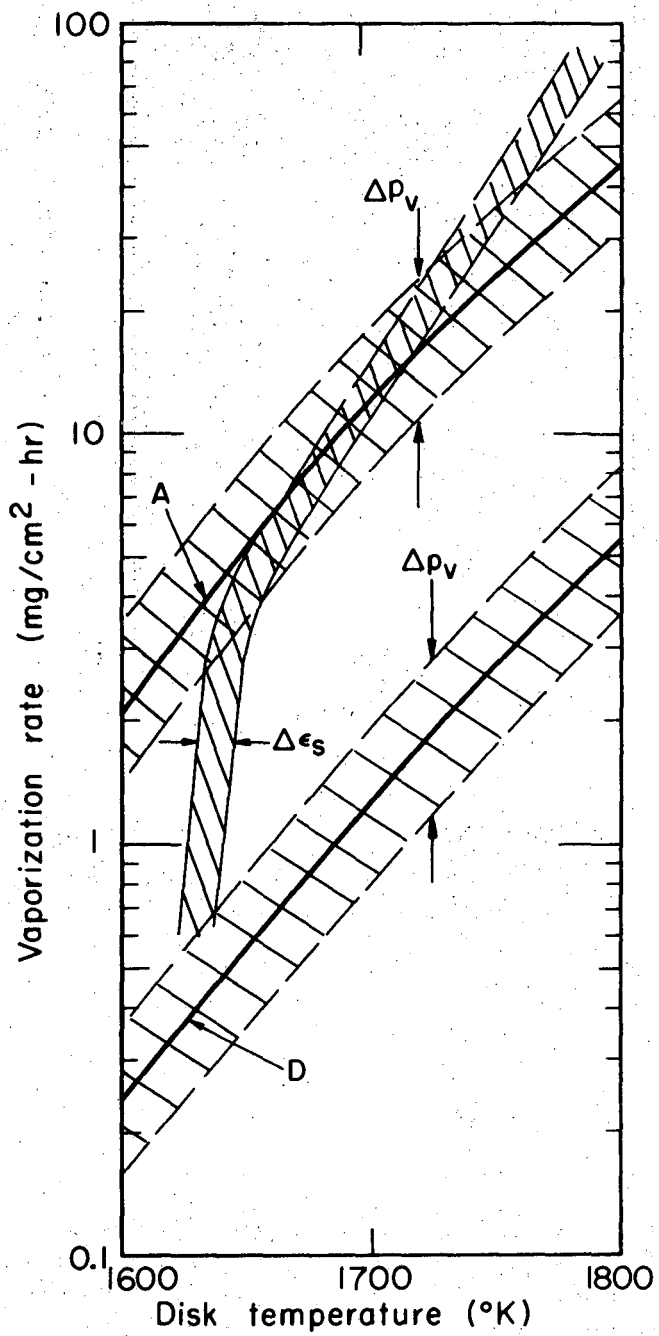
XBB698-5324

Fig. 5.



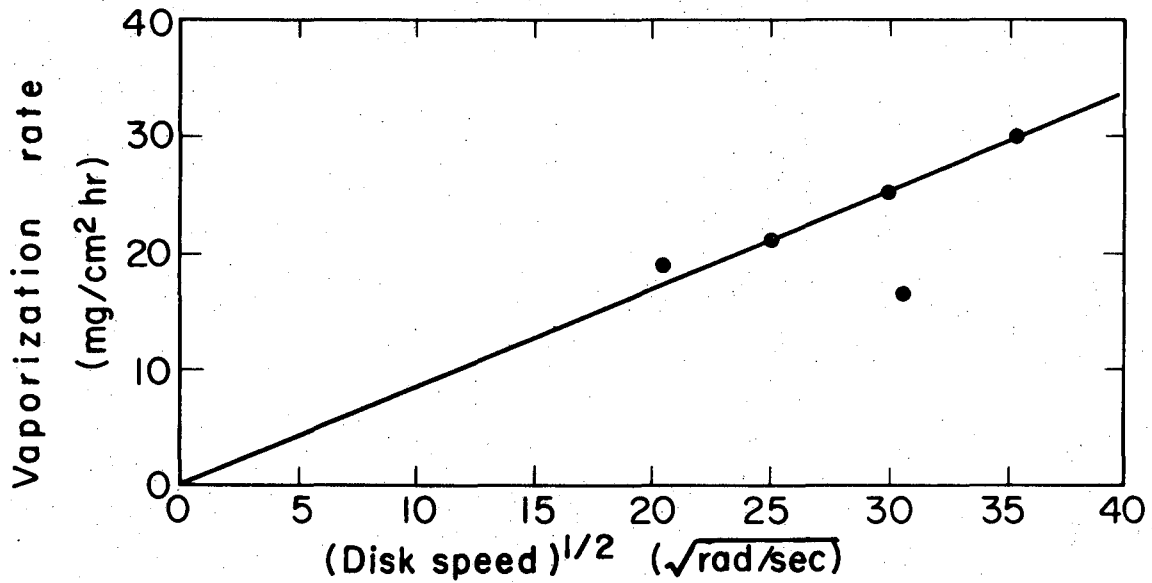
XBL 709 - 3918

Fig. 6.



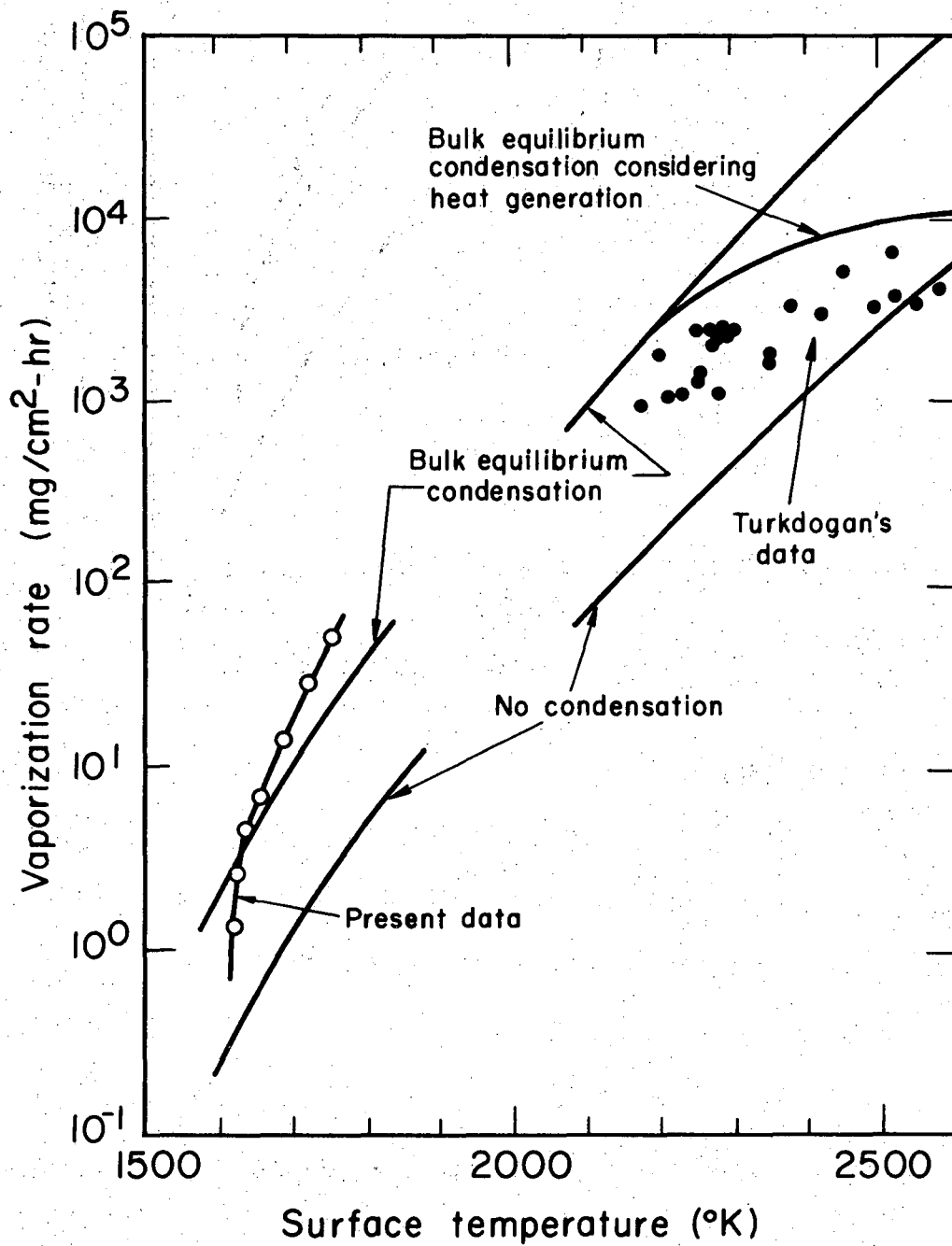
XBL709-3919

Fig. 7.



XBL699-3798

Fig. 8.



XBL709-3920

Fig. 9.

TABLE I

<u>Data Summary</u>						
<u>Run No.</u>	<u>Weight Loss (mg)</u>	<u>Time (min)</u>	<u>Speed (rpm)</u>	T_a^b <u>(°K)</u>	T_t^b <u>(°K)</u>	<u>Vaporization rate (mg/cm²-hr)</u>
1	6.61	10	12,000	1667	1759	48.9
2	0.93	50	12,000	1552	1631	1.38
3	10.28	50	12,000	1615	1701	15.2
4	5.54	60	12,000	1584	1667	6.83
5	8.04	20	12,000	1642	1731	29.8
6	4.24	60	12,000	1567	1648	5.23
7	2.26	60	12,000	1556	1636	2.79
8	4.45	20	9,000	1644	1733	16.5
9	12.7	45	6,000	1638	1727	20.9
10	15.4	60	4,200	1635	1723	19.0
11	10.2	30	8,400	1638	1727	25.2
12 ^a	7.21	15	12,000	1666	1758	35.6
13 ^a	8.46	45	12,000	1616	1702	14.0
14 ^a	6.52	20	12,000	1638	1727	24.1

^aNos. 12 and 13 were run with heater installed and on; No. 14 with heater installed but no power.

^b T_a is the apparent temperature of the disk, i.e., the observed temperature uncorrected for emissivity. T_t has been corrected for a surface emissivity of 0.50.

^cArea of the disk is 0.81 cm².

MEASUREMENT OF THE SURFACE EMISSIVITY AND TEMPERATURE

The procedure for determining the emissivity of the disk surface was as follows. A set of temperature measurements were made while the disk was being heated to and cooled from its operating temperature for the run. The measurements consisted of recording the temperature of the hole drilled in the disk and then the temperature of the surface immediately adjacent to the hole for a sequence of different disk temperatures. If an axial temperature gradient did not exist, the true temperature of the bottom of the hole would be equal to the true temperature of the surface*. The relationship between the true and apparent temperatures as seen by the optical pyrometer is²³:

$$\frac{1}{T_t} = \frac{1}{T_a} + \frac{\lambda}{C_2} \ln \epsilon \quad (A)$$

where λ is the 6500Å wavelength to which the pyrometer is sensitive and ϵ is the emissivity at this wavelength. C_2 is the second radiation constant of Planck's law. Eq(A) applies to both the disk hole and the surface. If the true hole and surface temperatures are equal, the ratio of the hole and surface emissivities is a function of the measured apparent temperatures only:

$$\frac{\epsilon_h}{\epsilon_s} = \exp \left[\frac{C_2}{\lambda} \left(\frac{1}{T_a^s} - \frac{1}{T_a^h} \right) \right] \quad (B)$$

* If an axial temperature gradient does exist, and a small one did in these measurements, the analysis becomes more complicated because the true hole and surface temperature differ by an amount determined by the axial temperature gradient. The relationships for this case are derived in Ref. (20).

where the superscripts h and s denote hole and surface temperature, respectively.

From the calculations of Sparrow, Albers and Eckert²⁴, the emissivity of the disk surface can be obtained by replotting the graphs in ref. 24 in the form[†]:

$$\epsilon_s = f\left(\frac{\epsilon_h}{\epsilon_s}, \frac{l}{d}\right) \quad (C)$$

where l/d is the length-to-diameter ratio of the hole. The two temperature measurements give the emissivity ratio by Eq(B). The surface emissivity is obtained from the plots represented by Eq(C).

This procedure was repeated for a sequence of different temperature levels and an average surface emissivity of 0.50 was obtained.²⁰ The data compiled in ref. 14 scatter widely, but the most reliable value is approximately 0.43.

Once the emissivity of the disk surface is known, the true surface temperature may be obtained from the apparent surface temperature and Eq(A).

[†] In calculating the surface emissivity by Eq(C), the effect of the local emissivity variation across the bottom of the hole was neglected and the emissivity at the bottom was assumed to be equal to the radial average. The error produced by this assumption should be negligible because the variation is small for holes with an $l/d = 1$, and also because the measured temperature attributed to the hole was the average value measured across the hole bottom.

LEGAL NOTICE

This report was prepared as an account of Government sponsored work. Neither the United States, nor the Commission, nor any person acting on behalf of the Commission:

- A. Makes any warranty or representation, expressed or implied, with respect to the accuracy, completeness, or usefulness of the information contained in this report, or that the use of any information, apparatus, method, or process disclosed in this report may not infringe privately owned rights; or*
- B. Assumes any liabilities with respect to the use of, or for damages resulting from the use of any information, apparatus, method, or process disclosed in this report.*

As used in the above, "person acting on behalf of the Commission" includes any employee or contractor of the Commission, or employee of such contractor, to the extent that such employee or contractor of the Commission, or employee of such contractor prepares, disseminates, or provides access to, any information pursuant to his employment or contract with the Commission, or his employment with such contractor.

TECHNICAL INFORMATION DIVISION
LAWRENCE BERKELEY LABORATORY
UNIVERSITY OF CALIFORNIA
BERKELEY, CALIFORNIA 94720